Inorg. Chem. **2005**, *44*, 2050–2059

$[Fe(bpb)(CN)_2]^-$ as a Versatile Building Block for the Design of Novel Low-Dimensional Heterobimetallic Systems: Synthesis, Crystal Structures, and Magnetic Properties of Cyano-Bridged Fe^{III}–Ni^{II} Complexes [$(bpb)^{2-}$ = 1,2-Bis(pyridine-2-carboxamido)benzenate]

Zhong-Hai Ni,[†] Hui-Zhong Kou,*[,†] Yi-Hua Zhao,[†] Lei Zheng,[†] Ru-Ji Wang,[†] Ai-Li Cui,[†] and Osamu Sato[‡]

Department of Chemistry, Tsinghua University, Beijing 100084, P. R. China, and Kanagawa Academy of Science and Technology, KSP Building, East 412, 3-2-1 Sakado, Takatsu-ku, Kawasaki-shi, Kanagawa 213-0012, Japan

Received July 27, 2004

A dicyano-containing $[Fe(bpb)(CN)_2]^-$ building block has been employed for the synthesis of cyano-bridged heterometallic Ni^{II}–Fe^{III} complexes. The presence of steric bpb^{2-} ligand around the iron ion results in the formation of low-dimensional species: five are neutral $NiFe_2$ trimers and three are one-dimensional (1D). The structure of the 1D complexes consists of alternating $[NiL]^{2+}$ and $[Fe(bpb)(CN)_2]^-$ generating a cyano-bridged cationic polymeric chain and the perchlorate as the counteranion. In all complexes, the coordination geometry of the nickel ions is approximately octahedral with the cyano nitrogen atoms at the trans positions. Magnetic studies of seven complexes show the presence of ferromagnetic interaction between the metal ions through the cyano bridges. Variable temperature magnetic susceptibility investigations of the trimeric complexes yield the following J_{NiFe} values (based on the spin exchange Hamiltonian $H = -2J_{NiFe}S_{Ni}(S_{Fe(1)} + S_{Fe(2)})$: J_{NiFe} = 6.40(5), 7.8(1), 8.9(2), and 6.03(4) cm^{-1}, respectively. The study of the magneto-structural correlation reveals that the cyanide-bridging bond angle is related to the strength of magnetic exchange coupling: the larger the Ni—N≡C bond angle, the stronger the Ni- - -Fe magnetic interaction. One 1D complex exhibits long-range antiferromagnetic ordering with T_N = 3.5 K. Below T_N (1.82 K), a metamagnetic behavior was observed with the critical field of ∼6 kOe. The present research shows that the $[Fe(bpb)(CN)_2]^-$ building block is a good candidate for the construction of low-dimensional magnetic materials.

Introduction

Magnetism of coordination compounds has been one of the most active fields in coordination chemistry. The main active research areas in this field include the synthesis of single-molecule magnets (SMMs)[1−7] and single-chain magnets (SCMs),[8−11] high-T_c magnetic materials[12−15] and magneto-optical or magneto-conductor multifunctional materials,[16−22]

* To whom correspondence should be addressed. E-mail: kouhz@mail.tsinghua.edu.cn. Fax: 86-10-62795477.

[†] Tsinghua University.

[‡] Kanagawa Academy of Science and Techology.

(1) Mironov, V. S.; Chibotaru, L. F.; Ceulemans, A. *J. Am. Chem. Soc.* **2003**, *125*, 9750.
(2) Boudalis, A. K.; Donnadieu, B.; Nastopoulos, V.; Clemente-Juan, J. M.; Mari, A.; Sanakis, Y.; Tuchagues, J.-P.; Perlepes, S. P. *Angew. Chem., Int. Ed.* **2004**, *43*, 2266.
(3) Berlinguette, C. P.; Vaughn, D.; Cañada-Vilalta, C.; Galán-Mascarós, J. R.; Dunbar, K. R. *Angew. Chem., Int. Ed.* **2003**, *42*, 1523.
(4) Sokol, J. J.; Hee, A. G.; Long, J. R. *J. Am. Chem. Soc.* **2002**, *124*, 7656.
(5) Soler, M.; Wernsdorfer, W.; Folting, K.; Pink, M.; Christou, G. *J. Am. Chem. Soc.* **2004**, *126*, 2156.
(6) Lescouëzec, R.; Vaissermann, J.; Ruiz-Pérez, C.; Lloret, F.; Carrasco, R.; Julve, M.; Verdaguer, M.; Dromzee, Y.; Gatteschi, D.; Wernsdorfer, W. *Angew. Chem., Int. Ed.* **2003**, *42*, 1483.
(7) Karasawa, S.; Zhou, G.; Morikawa, H.; Koga, N. *J. Am. Chem. Soc.* **2003**, *125*, 13676.
(8) Caneschi, A.; Gatteschi, D.; Lalioti, N.; Sangregorio, C.; Sessoli, R.; Venturi, G.; Vindigni, A.; Rettori, A.; Pini, M. G.; Novak, M. A. *Angew. Chem., Int. Ed.* **2001**, *40*, 1760.
(9) Clerac, R.; Miyasaka, H.; Yamashita, M.; Coulon, C. *J. Am. Chem. Soc.* **2002**, *124*, 12837.
(10) Liu, T.-F.; Fu, D.; Gao, S.; Zhang, Y.-Z.; Sun, H.-L.; Su, G.; Liu, Y.-J. *J. Am. Chem. Soc.* **2003**, *125*, 13976.
(11) Wang, S.; Zuo, J.-L.; Gao, S.; Song, Y.; Zhou, H.-C.; Zhang, Y.-Z.; You, X.-Z. *J. Am. Chem. Soc.* **2004**, *126*, 8900.
(12) Holmes, S. M.; Girolami, G. S. *J. Am. Chem. Soc.* **1999**, *121*, 5593.
(13) Hatlevik, O.; Buschmann, W. E.; Manson, J. L.; Miller, J. S. *Adv. Mater.* **1999**, *11*, 914.
(14) Kou, H.-Z.; Gao, S.; Zhang, J.; Wen, G.-H.; Su, G.; Zheng, R. K.; Zhang, X. X. *J. Am. Chem. Soc.* **2001**, *123*, 11809.

10.1021/ic0489903 CCC: $30.25
Published on Web 02/16/2005

spin-crossover (SCO) materials[23−25] and materials with new magnetic phenomena,[26] nanosized molecular magnetic materials,[27,28] and paramagnetic complexes for the investigation of the magneto-structural correlation.

Several strategies have been developed in the past two decades for cyano-bridged complexes with the above-mentioned magnetic properties. Initially, the use of the hexacyanometalate unit $[M(CN)_6]^{q-}$ (M = Fe, Cr, Mn, or V) as a paramagnetic building block toward hydrated paramagnetic 3d metal ions $[M'(H_2O)_6]^{p+}$ has provided a large family of three-dimensional compounds known as Prussian blue analogues, some of which exhibit critical temperatures (T_c) as high as 310 K,[12] negative magnetization,[26] and magneto-conductor properties.[16] However, single crystals of these highly insoluble three-dimensional complexes for X-ray structural analysis are very difficult to grow,[29] which makes both the determination of the crystallographic structure and the interpretation of the magnetic behaviors difficult. Subsequently, another novel synthetic strategy has been widely used based also on $[M(CN)]_6^{q-}$ as a building block but reacting with the coordinatively unsaturated complexes $[M'(L)_x(H_2O)_y]^{p+}$, where L stands for an organic ligand. The incorporation of different polydentate ligands should give rise to new types of complexes called hybrid Prussian blue analogues. It can be further anticipated that the magnetism of such complexes should be modified accordingly. Successfully, a few high-spin clusters[30−40] and a series of one-,[41−46] two-,[47−49] and three-dimensional[14,15,50] cyanide-bridged bimetallic polymers that exhibit SMM, SCM, SCO, metamagnetism, and high-T_c have been obtained. Recently, one other new strategy for assembling cyanide-bridged complexes has been developed in order to control the dimensionality of the desired complexes with novel magnetic properties. This is based on the introduction of changeable versatile building blocks $[M(L)_x(CN)_y]^{q-}$ (L represents a blocking ligand). Although there are only a few stable cyano-containing building blocks that have been synthesized and explored in assembling cyano-bridged complexes, this strategy has yielded a variety of structures over a wide range of dimensionalities, including molecular clusters,[51−55] 1D chains,[56−59] and 2D layered networks.[60,61]

(15) Ohba, M.; Usuki, N.; Fukita, N.; Okawa, H. *Angew. Chem., Int. Ed*. **1999**, *38*, 1795.
(16) Sato, O.; Iyoda, T.; Fujishima, A.; Hashimoto, K. *Science* **1996**, *272*, 704. Sato, O.; Kawakami, T.; Kimura, M.; Hishiya, S.; Kubo, S.; Einaga, Y. *J. Am. Chem. Soc.* **2004**, *126*, 13176.
(17) Moore, J. G.; Lochner, E. J.; Ramsey, C.; Dalal, N. S.; Stiegman, A. E. *Angew. Chem., Int. Ed*. **2003**, *42*, 2741.
(18) Llusar, R.; Uriel, S.; Vicent, C.; Clemente-Juan, J. M.; Coronado, E.; Gómez-García, C. J.; Braida, B.; Canadell, E. *J. Am. Chem. Soc*. **2004**, *126*, 12076.
(19) Coronado, E.; Gómez-García, C. J.; Nuez, A.; Romero, F. M.; Rusanov, E.; Stoeckli-Evans, H. *Inorg. Chem*. **2002**, *41*, 4615.
(20) Inoue, K.; Imai, H.; Ghalsasi, P. S.; Kikuchi, K.; Ohba, M.; Okawa, H.; Yakhmi, J. V. *Angew. Chem., Int. Ed*. **2001**, *40*, 4242.
(21) Carbonera, C.; Dei, A.; Letard, J.-F.; Sangregorio, C.; Sorace, L. *Angew. Chem., Int. Ed*. **2004**, *43*, 3136.
(22) Coronado, E.; Galan-Mascaros, J. R.; Gómez-García, C. J.; Laukhin, V. *Nature* **2000**, *408*, 447.
(23) Berlinguette, C. P.; Dragulescu-Andrasi, A.; Sieber, A.; Galan-Mascaros, J. R.; Gudel, H.-U.; Achim, C.; Dunbar, K. R. *J. Am. Chem. Soc.* **2004**, *126*, 6222.
(24) Halder, G. J.; Kepert, C. J.; Moubaraki, B.; Murray, K. S.; Cashion, J. D. *Science* **2002**, *298*, 1763.
(25) Goodwin, H. A. T. *Top. Curr. Chem*. **2004**, *233*, 59. Long, G. J.; Grandjean, F.; Reger, D. L. *Top. Curr. Chem*. **2004**, *233*, 91. van Koningsbruggen, P. J. *Top. Curr. Chem*. **2004**, *233*, 123. Toftlund, H.; McGarvey, J. J. *Top. Curr. Chem*. **2004**, *233*, 151. Murray, K. S.; Kepert, C. J. *Top. Curr. Chem*. **2004**, *233*, 195. Garcia, Y.; Niel, V.; Muñoz, M. C.; Real, J. A. *Top. Curr. Chem*. **2004**, *233*, 229. van Koningsbruggen, P. J.; Maeda, Y.; Oshio, H. *Top. Curr. Chem*. **2004**, *233*, 259.
(26) Tokoro, H.; Ohkoshi, S.-i.; Matsuda, T.; Hashimoto, K. *Inorg. Chem*. **2004**, *43*, 5231. Ohkoshi, S.-i.; Abe, Y.; Fujishima, A.; Hashimoto, K. *Phys. Rev. Lett.* **1999**, *82*, 1285.
(27) Dujardin, E.; Mann, S. *Adv. Mater*. **2004**, *16*, 1125 and references therein.
(28) Conia, A.; Fabretti, A. C.; Pacchioni, M.; Zobbi, L.; Bonacchi, D.; Caneschi, A.; Gatteschi, D.; Biagi, R.; Pennino, U. D.; Renzi, V. D.; Gurevich, L.; Van der Zant, H. S. J. *Angew. Chem., Int. Ed*. **2003**, *42*, 1645.
(29) Dong, W.; Zhu, L.-N.; Song, H.-B.; Liao, D.-Z.; Jiang, Z.-H.; Yan, S.-P.; Cheng, P.; Gao, S. *Inorg. Chem*. **2004**, *43*, 2465.
(30) Choi, H. J.; Sokol, J. J.; Long, J. R. *Inorg. Chem*. **2004**, *43*, 1606.
(31) Fu, D. G.; Chen, J.; Tan, X. S.; Jiang, L. J.; Zhang, S. W.; Zheng, P. J.; Tang, W. X. *Inorg. Chem*. **1997**, *36*, 220.
(32) Si, S.-F.; Tang, J.-K.; Liu, Z.-Q.; Liao, D.-Z.; Jiang, Z.-H.; Yan, S.-P.; Cheng, P. *Inorg. Chem. Commun.* **2003**, *6*, 1109.
(33) Marvaud, V.; Decroix, C.; Scuiller, A.; Guyard-Duhayon, C.; Vaissermann, J.; Gonnet, F.; Verdaguer, M. *Chem.—Eur. J*. **2003**, *9*, 1678.
(34) Herchel, R.; Boca, R.; Gembicky, M.; Kozisek, J.; Renz, F. *Inorg. Chem*. **2004**, *43*, 4103.
(35) Vostrikova, K. E.; Luneau, D.; Wernsdorfer, W.; Rey, P.; Verdaguer, M. *J. Am. Chem. Soc*. **2000**, *122*, 718.
(36) Parker, R. J.; Spiccia, L.; Berry, K. J.; Fallon, G. D.; Moubaraki, B.; Murray, K. S. *Chem. Commun*. **2001**, 333. Tanase, S.; Andruh, M.; Stanica, N.; Mathoniere, C.; Rombaut, G.; Golhen, S.; Ouahab, L. *Polyhedron* **2003**, *22*, 1315.
(37) Parker, R. J.; Lu, K. D.; Batten, S. R.; Moubaraki, B.; Murray, K. S.; Spiccia, L.; Cashion, J. D.; Rae, A. D.; Willis, A. C. *J. Chem. Soc., Dalton Trans*. **2002**, 3723. Kou, H.-Z.; Zhou, B. C.; Si, S.-F.; Wang, R.-J. *Inorg. Chem*. **2004**, *43*, 401.
(38) Van Langenberg, K.; Batten, S. R.; Berry, K. J.; Hockless, D. C. R.; Moubaraki, B.; Murray, K. S. *Inorg. Chem*. **1997**, *36*, 5006.
(39) Kou, H.-Z.; Zhou, B. C.; Liao, D.-Z.; Wang, R.-J.; Li, Y. *Inorg. Chem.* **2002**, *41*, 6887.
(40) Berlinguette, C. P.; Galan-Mascaros, J. R.; Dunbar, K. R. *Inorg. Chem*. **2003**, *42*, 3416.
(41) Fallah, M. S. E.; Ribas, J.; Solans, X.; Font-Bardia, M. *J. Chem. Soc., Dalton Trans*. **2001**, 247. Shen, X.; Li, B.; Zou, J.; Xu, Z. *Transition Met. Chem.* (*Dordrecht, Neth.*) **2002**, *27*, 372. El Fallah, M. S.; Ribas, J.; Solans, X.; Font-Bardia, M. *New J. Chem.* **2003**, *27*, 895.
(42) Colacio, E.; Dominguez-Vera, J. M.; Ghazi, M.; Kivekas, R.; Klinga, M.; Moreno, J. M. *Chem. Commun*. **1998**, 1071.
(43) Kou, H.-Z.; Zhou, B. C.; Gao, S.; Liao, D.-Z.; Wang, R.-J. *Inorg. Chem*. **2003**, *42*, 5604.
(44) Ohba, M.; Usuki, N.; Fukita, N.; Okawa, H. *Inorg. Chem*. **1998**, *37*, 3349.
(45) Colacio, E.; Dominguez-Vera, J. M.; Lloret, F.; Rodriguez, A.; Stoeckli-Evans, H. *Inorg. Chem*. **2003**, *42*, 6962.
(46) Miyasaka, H.; Ieda, H.; Matsumoto, N.; Re, N.; Crescenzi, R.; Floriani, C. *Inorg. Chem*. **1998**, *37*, 255.
(47) Smith, J. A.; Galán-Mascarós, J.-R.; Clérac, R.; Dunbar, K. R. *Chem. Commun*. **2000**, 1077.
(48) Thétiot, F.; Triki, S.; Pala, J. S.; Gómez-García, C. J.; Golhen, S. *Chem. Commun.* **2002**, 1078.
(49) Marvilliers, A.; Parsons, S.; Riviere, E.; Audiere, J. P.; Kurmoo, M.; Mallah, T. *Eur. J. Inorg. Chem*. **2001**, 1287.
(50) El Fallah, M. S.; Rentschler, E.; Caneschi, A.; Sessoli, R.; Gatteschi, D. *Angew. Chem., Int. Ed. Engl*. **1996**, *35*, 1947.
(51) Sokol, J. J.; Shores, M. P.; Long, J. R. *Angew. Chem., Int. Ed*. **2001**, *40*, 236.
(52) Oshio, H.; Onodera, H.; Ito, T. *Chem.—Eur. J*. **2003**, *9*, 3946.
(53) Wang, S.; Zuo, J.-L.; Zhou, H.-C.; Song, Y.; Gao, S.; You, X.-Z. *Eur. J. Inorg. Chem.* **2004**, 3681. Kim, J.; Han, S.; Cho, I.-K.; Choi, K. Y.; Heu, M.; Yoon, S.; Duh, B. J. *Polyhedron* **2004**, *23*, 1333.
(54) Lescouëzec, R.; Lloret, F.; Julve, M.; Vaissermann, J.; Verdaguer, M. *Inorg. Chem*. **2002**, *41*, 818.
(55) Yang, J. Y.; Shores, M. P.; Sokol, J. J.; Long, J. R. *Inorg. Chem*. **2003**, *42*, 1403.
(56) Toma, L. M.; Delgado, F. S.; Ruiz-Perez, C.; Carrasco, R.; Cano, J.; Lloret, F.; Julve, M. *J. Chem. Soc., Dalton Trans*. **2004**, 2836.

Scheme 1. Schematic Illustration of the Polyaza Ni(II) Building Blocks

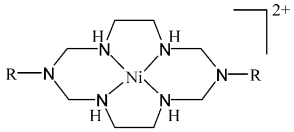

$[NiL^n]^{2+}$ (R = CH_3 (L^1), CH_3CH_2 (L^2), $HOCH_2CH_2$ (L^3) and $C_6H_5CH_2CH_2$ (L^4))

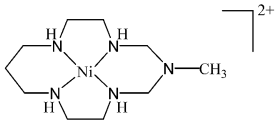

$[NiL^5]^{2+}$ (L^5 = 3-methyl-1,3,5,8,12-pentaazacyclotetradecane)

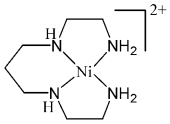

$[NiL^6]^{2+}$ (L^6 = 1,9-diamino-3,7-diazanonane (2,3,2-tet))

This indicates that this strategy seems very promising in designing novel cyano-bridged complexes with desired structures and/or magnetic properties, especially low-dimensional heterobimetallic systems.

Albeit few, cyano-bridged polynuclear complexes have been synthesized in order to investigate the magneto-structural correlations because it is facile to find a model to evaluate the magnitude of intermetallic magnetic coupling. We focused on dicyano-containing metal complexes and first explored the use of $[Fe(bpb)(CN)_2]^-$ as a building block. We presume that the presence of a rigid, bulky, and planar bpb^{2-} ligand favors the formation of polynuclear or one-dimensional species. In this work, we present our first attempt which concerns the synthesis, crystal structures, and magnetic properties of the complexes $[NiL^1][Fe(bpb)(CN)_2]_2 \cdot H_2O$ (**1**), $[NiL^3][Fe(bpb)(CN)_2]_2 \cdot 7H_2O$ (**3**), $[NiL^4][Fe(bpb)(CN)_2]_2 \cdot 4H_2O$ (**4**), $[NiL^5][Fe(bpb)(CN)_2]_2$ (**5**), $[NiL^6][Fe(bpb)(CN)_2](ClO_4) \cdot CH_3OH$ (**6**), $[NiL^1][Fe(bpb)(CN)_2](ClO_4) \cdot H_2O$ (**7**), and $[NiL^4][Fe(bpb)(CN)_2](ClO_4) \cdot 2CH_3CN$ (**8**), together with the crystal structure of $[NiL^2][Fe(bpb)(CN)_2]_2 \cdot 6H_2O$ (**2**). The polyaza-Ni(II) complexes employed in the experiments are shown in Scheme 1.

Experimental Section

Elemental analyses of carbon, hydrogen, and nitrogen were carried out with an Elementary Vario El. The infrared spectroscopy on KBr pellets was performed on a Magna-IR 750 spectrophotometer in the 4000−400 cm^{-1} region. Variable-temperature magnetic susceptibility, zero-field ac magnetic susceptibility, and field dependence magnetization measurements were performed on a Quantum Design MPMS SQUID magnetometer. The experimental susceptibilities were corrected for the diamagnetism of the constituent atoms (Pascal's tables).

Syntheses. The precursors $[NiL^1](ClO_4)_2$,[62] $[NiL^2](ClO_4)_2$,[62] $[NiL^3](ClO_4)_2$,[63] $[NiL^4](ClO_4)_2$,[64] $[NiL^5](ClO_4)_2$,[65] $[NiL^6](ClO_4)_2$,[66] and $K[Fe(bpb)(CN)_2]$[67] were prepared according to literature methods. **Caution!** Perchlorate salts of metal complexes with organic ligands are potentially explosive and should be handled in small quantities with care.

$[NiL^1][Fe(bpb)(CN)_2]_2 \cdot H_2O$ (1), $[NiL^3][Fe(bpb)(CN)_2]_2 \cdot 7H_2O$ (3), $[NiL^4][Fe(bpb)(CN)_2]_2 \cdot 4H_2O$ (4), and $[NiL^5][Fe(bpb)(CN)_2]_2$ (5). Because complexes **1**, **3**, **4,** and **5** were prepared similarly, a representative method for complex **1** is described. Black block single crystals of **1** were obtained at room temperature by the slow diffusion of yellow acetonitrile and an aqueous solution (5 mL) of $[NiL^1](ClO_4)_2$ (0.1 mmol, 50.5 mg) into a dark green methanol solution (5 mL) of $K[Fe(bpb)(CN)_2]$ (0.1 mmol, 46.1 mg) for about 1 week. These crystals were collected carefully and air-dried. Yield: 22−42 mg (40−60%).

$[NiL^2][Fe(bpb)(CN)_2]_2 \cdot 6H_2O$ (2). Only a few black block crystals of **2** were obtained by using the above-described method, one of which was selected and subjected to X-ray diffraction analysis.

$[NiL^6][Fe(bpb)(CN)_2](ClO_4) \cdot CH_3OH$ (6). Uniform black block single crystals of the complex were obtained at room temperature by evaporation of the $CH_3CN-H_2O-MeOH$ solution of $[Ni(L^6)](ClO_4)_2$ (0.1 mmol) and $K[Fe(bpb)(CN)_2]$ (0.1 mmol) for about 2 days. Yield: 21.5 mg (27.8%).

$[NiL^1][Fe(bpb)(CN)_2](ClO_4)$ (7) and $[NiL^4][Fe(bpb)(CN)_2](ClO_4) \cdot 2CH_3CN$ (8). Black strip crystals of complexes **7** and **8** suitable for X-ray structure analysis were grown in a sealed beaker or a single tube at room temperature by carefully mixing a CH_3CN-H_2O solution of $[Ni(L^1)](ClO_4)_2$ or $[Ni(L^4)](ClO_4)_2$ (0.1 mmol) and $K[Fe(bpb)(CN)_2]$ (0.1 mmol) in MeOH for about 2 days. Yield: 41.0 mg (50%) for **7** and 29.8 mg (27.7%) for **8**.

Anal. Calcd for $NiFe_2C_{50}H_{52}N_{18}O_5$ (**1**): C, 51.97; H, 4.54; N, 21.82. Found: C, 52.10; H, 4.66; N, 21.46. Selected IR frequencies (KBr disk, cm^{-1}): 2140 (s, $\upsilon_{C\equiv N}$), 2116 (s, $\upsilon_{C\equiv N}$), 1615 (vs, $\upsilon_{C=O}$), 1591 (vs), 1470 (s), 1362 (s), 1141 (s), 761 (s), 747 (s), 690 (m), 506 (m).

Anal. Calcd for $NiFe_2C_{52}H_{68}N_{18}O_{13}$ (**3**): C, 47.19; H, 5.18; N, 19.05. Found: C, 46.80; H, 5.29; N, 18.95. Selected IR frequencies (KBr disk, cm^{-1}): 2147 (m, $\upsilon_{C\equiv N}$), 2131 (m, $\upsilon_{C\equiv N}$), 1609 (s, $\upsilon_{C=O}$), 1587 (vs), 1468 (m), 1357 (s), 1141 (m), 758 (s), 690 (w).

Anal. Calcd for $NiFe_2C_{64}H_{70}N_{18}O_8$ (**4**): C, 55.31; H, 5.08; N, 18.14. Found: C, 55.78; H, 5.12; N, 18.58. Selected IR frequencies (KBr disk, cm^{-1}): 2159 (m, $\upsilon_{C\equiv N}$), 2118 (m, $\upsilon_{C\equiv N}$), 1612 (vs, $\upsilon_{C=O}$), 1589 (vs), 1470 (s), 1363 (s), 1141 (m), 755 (s), 690 (m), 506 (m).

Anal. Calcd for $NiFe_2C_{50}H_{49}N_{17}O_4$ (**5**): C, 53.50; H, 4.40; N, 21.21. Found: C, 52.98; H, 4.52; N, 21.34. Selected IR frequencies

(57) Matsumoto, N.; Sunatsuki, Y.; Miyasaka, H.; Hashimoto, Y.; Luneau, D.; Tuchagues, J.-P. *Angew. Chem., Int. Ed.* **1999**, *38*, 171.
(58) Lescouëzec, R.; Lloret, F.; Julve, M.; Vaissermann, J.; Verdaguer, M.; Llusar, R.; Uriel, S. *Inorg. Chem.* **2001**, *40*, 2065.
(59) Lescouëzec, R.; Vaissermann, J.; Toma, L. M.; Carrasco, R.; Lloret, F.; Julve, M. *Inorg. Chem.* **2004**, *43*, 2234.
(60) Yeung, W.-F.; Man, W.-L.; Wong, W.-T.; Lau, T.-C.; Gao, S. *Angew. Chem., Int. Ed.* **2001**, *40*, 3031.
(61) Zhang, Y.-Z.; Gao, S.; Sun, H.-L.; Su, G.; Wang, Z.-M.; Zhang, S. W. *Chem. Commun.* **2004**, 1906.
(62) Suh, M. P.; Kang, S.-G. *Inorg. Chem.* **1988**, *27*, 2544.
(63) Hay, R. W.; Armstrong, J. M.; Hassan, M. M. *Transition Met. Chem. (Dordrecht, Neth.)* **1992**, *17*, 270.
(64) Lu, T.-B.; Xiang, H.; Li, X.; Mao, Z.; Ji, L. *Inorg. Chem. Commun.* **2000**, *3*, 597.
(65) Cromie, T. J.; Hay, R. W.; Lightfoot, P.; Richens, D. T.; Crayston, J. A. *Polyhedron* **2001**, *20*, 307.
(66) Bernard, B. R.; Haines, R. I.; Rowley, J. E. *Transition Met. Chem. (Dordrecht, Neth.)* **2001**, *26*, 164.
(67) Ray, M.; Mukherjee, R.; Richardson, J. F.; Buchanan, R. M. *J. Chem. Soc., Dalton Trans.* **1993**, 2451. Dutta, S. K.; Beckmann, U.; Bill, E.; Weyhermuller, T.; Wieghardt, K. *Inorg. Chem.* **2000**, *39*, 3355.

(KBr disk, cm^{-1}): 2140 (m, $\nu_{C\equiv N}$), 2119 (m, $\nu_{C\equiv N}$), 1613 (s, $\nu_{C=O}$), 1590 (vs), 1470 (s), 1362 (s), 1141 (m), 745 (m), 689 (m), 506 (m).

Anal. Calcd for $NiFeC_{28}H_{36}ClN_{10}O_7$ (**6**): C, 43.41; H, 4.68; N, 18.08. Found: C, 43.42; H, 4.77; N, 18.19. Selected IR frequencies (KBr disk, cm^{-1}): 2146 (s, $\nu_{C\equiv N}$), 1634 (s, $\nu_{C=O}$), 1594 (vs), 1472 (m), 1358 (s), 1139 (m), 1084 (vs, ν_{Cl--O}), 751 (m), 623 (m), 505 (w).

Anal. Calcd for $NiFeC_{30}H_{38}ClN_{12}O_6$ (**7**): C, 44.34; H, 4.71; N, 20.68. Found: C, 44.05; H, 4.87; N, 20.62. Selected IR frequencies (KBr disk, cm^{-1}): 2139 (m, $\nu_{C\equiv N}$), 1614 (s, $\nu_{C=O}$), 1589 (vs), 1471 (s), 1363 (s), 1142 (m), 1089 (vs, ν_{Cl-O}), 763 (m), 625 (m), 508 (m).

Anal. Calcd for $NiFeC_{48}H_{56}ClN_{14}O_6$ (**8**): C, 53.63; H, 5.25; N, 18.24. Found: C, 53.12; H, 5.24; N, 17.55. Selected IR frequencies (KBr disk, cm^{-1}): 2134 (m, $\nu_{C\equiv N}$), 1623 (s, $\nu_{C=O}$), 1592 (vs), 1472 (m), 1355 (s), 1139 (m), 1092 (vs, ν_{Cl-O}), 760 (m), 623 (m), 506 (w).

X-ray Structure Determination. The crystal data are summarized in Table 1. The structures were solved by the direct method (SHELXS-97) and refined by full-matrix least-squares (SHELXL-97) on F^2. Anisotropic thermal parameters were used for the non-hydrogen atoms and isotropic parameters for the hydrogen atoms. Hydrogen atoms were added geometrically and refined using a riding model. The methyl group in ligand L^5 in complex **5** experiences disorder over two positions due to the presence of an inversion center at the nickel atom. The occupancy factors of two sets of disordered atoms [N(9) and C(26)] were 0.5. In complex **7**, some atoms of the macrocycle around Ni(2) display some degree of disorder, and the DFIX command has been used. The R1 value of the data for complex **7** is high due to the weak diffraction of the single crystal; however, the bond distances around the metal ions are accurate enough for magneto-structural correlation analysis.

Results and Discussion

Synthesis and General Characterization. The eight complexes were reproducibly synthesized by the reactions of equivalent molar polyaza $[NiL^n](ClO_4)_2$ ($n = 1-6$) complexes with $K[Fe(bpb)(CN)_2]$. Interestingly, three of the obtained complexes are 1D chainlike complexes and the other five are trimers with similar Fe(III)−Ni(II)−Fe(III) sandwichlike structures. It is important to note that the three 1D chains are obtained by direct mixing of $[NiL^n](ClO_4)_2$ and $K[Fe(bpb)(CN)_2]$, whereas the five trimers are obtained by the slow diffusion of $[NiL^n](ClO_4)_2$ into the solution of $K[Fe(bpb)(CN)_2]$. Therefore, it is intriguing to note that the structures of the complexes strongly depend on the reaction condition employed.

The IR spectra of **1**−**5** in the range 2110−2160 cm^{-1} exhibit two sharp peaks assigned to cyano-stretching absorptions, indicating the presence of bridging and nonbridging cyano ligands in $[Fe(bpb)(CN)_2]^-$. Moreover, the bridging cyano groups usually absorb at a higher frequency than the terminal groups. For complexes **6**, **7**, and **8**, the strong broad peaks centered at 1090 cm^{-1} suggest the presence of ClO_4^- anions in these complexes, and the broad single peak between 2130 and 2150 cm^{-1} is assigned to the bridging cyano groups.

Crystal Structures. The eight complexes have been characterized by single-crystal X-ray diffraction. The stick

Table 1. Crystallographic Data for Complexes **1**–**8**

	1	**2**	**3**	**4**	**5**	**6**	**7**	**8**
chemical formula	$NiFe_2C_{50}H_{52}N_{18}O_5$	$NiFe_2C_{52}H_{66}N_{18}O_{10}$	$NiFe_2C_{52}H_{68}N_{18}O_{13}$	$NiFe_2C_{64}H_{70}N_{18}O_8$	$NiFe_2C_{50}H_{49}N_{17}O_4$	$NiFeC_{28}H_{36}ClN_{10}O_7$	$NiFeC_{30}H_{38}ClN_{12}O_6$	$NiFeC_{48}H_{56}ClN_{14}O_6$
fw	1155.51	1273.64	1323.65	1389.79	1122.47	774.68	812.73	1075.08
T (K)	293	293	293	293	293	293	293	293
cryst syst	monoclinic	triclinic	triclinic	monoclinic	monoclinic	monoclinic	triclinic	triclinic
space group	$C2/c$	$\bar{P}1$	$\bar{P}1$	$P2_1/c$	$P2_1/c$	$P2_1/c$	$\bar{P}1$	$\bar{P}1$
a (Å)	31.208(7)	9.0120(18)	9.0907(18)	14.181(2)	14.063(3)	8.4780(17)	10.530(2)	12.031(3)
b (Å)	13.545(4)	12.754(3)	12.861(3)	10.490(2)	13.440(3)	19.437(4)	13.456(3)	15.177(4)
c (Å)	13.043(4)	15.216(3)	15.096	24.058(5)	13.153(3)	20.664(4)	13.858(3)	15.386(4)
α (deg)	90	114.37(3)	113.48(3)	90	90	90	80.41(3)	106.197(16)
β (deg)	110.037(10)	93.67(3)	93.39(3)	104.203(14)	94.13(3)	93.50(3)	72.78(3)	94.706(17)
γ (deg)	90	105.56(3)	106.71(3)	90	90	90	81.81(3)	107.583(17)
V (Å^3)	5180(2)	1503.9(5)	1519.8(5)	3469.5(12)	2479.5(9)	3398.8(12)	1840.3(6)	2528.9(10)
Z	4	1	1	2	2	4	2	2
ρ_{calcd} (g cm^{-1})	1.482	1.406	1.446	1.330	1.503	1.514	1.467	1.412
F (000)	2392	664	690	1448	1160	1604	842	1122
data/restraints/params	4612/0/349	5807/0/382	10759/0/394	6091/0/425	4361/0/340	12566/0/433	6390/15/458	8731/0/643
R1 [$I > 2\sigma(I)$]	0.0897	0.0588	0.0600	0.0716	0.0607	0.0614	0.1109	0.0695
wR2 (all data)	0.2455	0.1303	0.1509	0.1707	0.1128	0.1403	0.2741	0.1704

Table 2. Selected Bond Distances (Å) and Angles (deg) for Complexes **1**−**5**

	1	**2**	**3**	**4**	**5**
Ni−N(2)	2.096(6)	2.082(4)	2.090(3)	2.066(6)	2.106(2)
Ni−N(7)	2.063(6)	2.062(3)	2.060(2)	2.069(5)	2.064(2)
Ni−N(8)	2.066(6)	2.057(4)	2.059(2)	2.085(5)	2.075(2)
Fe−C(1)	1.957(7)	1.955(4)	1.962(3)	1.963(7)	1.968(3)
Fe−C(2)	1.961(8)	1.958(4)	1.959(3)	1.945(7)	1.977(3)
Fe−N(3)	1.887(6)	1.879(3)	1.892(2)	1.890(5)	1.892(2)
Fe−N(4)	1.891(6)	1.892(2)	1.885(2)	1.884(5)	1.886(2)
Fe−N(5)	2.017(7)	1.997(3)	2.000(2)	2.002(5)	2.013(2)
Fe−N(6)	1.982(6)	1.986(3)	1.993(2)	1.994(5)	2.001(2)
Ni···Fe	5.093	5.091	5.110	5.133	5.068
C(2)−N(2)−Ni	160.2(7)	165.3(4)	163.2(2)	173.4(5)	157.0(2)
Fe−C(1)−N(1)	179.3(7)	178.7(4)	178.5(3)	174.4(6)	177.2(3)
Fe−C(2)−N(2)	172.2(7)	172.4(4)	173.6(3)	177.2(6)	172.1(3)
C(1)−Fe−C(2)	172.5(3)	173.75(15)	173.02(11)	167.2(3)	170.01(11)

and ball drawings of compounds **1**−**5** are shown in Figure 1, and selected bond distances and angles for complexes **1**−**5** are listed in Table 2. Crystal structures and selected bond distances and angles of complexes **6**−**8** are shown in Figure 2 and Table 3, respectively.

Crystal Structures of Trimers. The five complexes have similar sandwichlike structures made up of neutral trinuclear entities of general formula $[Fe(bpb)(CN)_2]_2[NiL^n]$ ($n = 1-5$), where each $[Fe(bpb)(CN)_2]^-$ unit acts as a monodentate ligand through one of its two cyanide groups toward the central Ni(II) ion.

The iron(III) ion in complexes **1**−**5** is coordinated by four bpb^{2-} nitrogen atoms and two cyanide carbon atoms, in a slightly distorted octahedral geometry. The Fe−C(1) (unbridging cyano) and Fe−C(2) (bridging cyano) bond distances of 1.968(3) Å and 1.977(3) Å for complex **5** are slightly larger than those of 1.955(4)−1.963(7) Å and 1.945(7)−1.961(3) Å for **1**−**4**. The iron atom and terminal cyanide in these complexes, except for **4**, are almost linear (177.2(3)−179.3(7)°), whereas the Fe−C≡N angles for the bridging cyanides are somewhat bent (172.1(3)−173.6(3)°). However, the Fe−C≡N angle for the bridging cyano group (177.2(6)°) in complex **4** is somewhat larger than that of the corresponding terminal cyano group (174.4(6)°).

The nickel atom is hexacoordinated with two cyanide nitrogen atoms at trans positions and four nitrogen atoms from the L^n ligand, yielding a NiN_6 octahedral surrounding. The Ni−N_{cyano} bond distances increase in the order **4** (2.066(2) Å) < **2** (2.082(4) Å) < **3** (2.090(3) Å) < **1** (2.096(6) Å) < **5** (2.106(2) Å), and the corresponding Ni−N≡C bond angles decrease in the order **4** (173.4(5)°) > **2** (165.3(4)°) > **3** (163.2(2)°) > **1** (160.2(7)°) > **5** (157.0(2)°). The intramolecular Fe- - -Ni separations through bridging cyanides are 5.093 Å for **1**, 5.091 Å for **2**, 5.110 Å for **3**, 5.133 Å for **4**, and 5.068 Å for **5**. The shortest intermolecular metal−metal distances are 6.580 Å for **1**, 6.630 Å for **2**, 6.558 Å for **3**, and 6.632 Å for **4** but are significantly different from that of **5** (7.786 Å).

Comparing the structure data of the five trimeric complexes, we found that the Ni−N≡C bond angles, the Ni−N_{cyano} bond distances, and the intramolecular Fe- - -Ni separations have some dependence; that is, the larger the

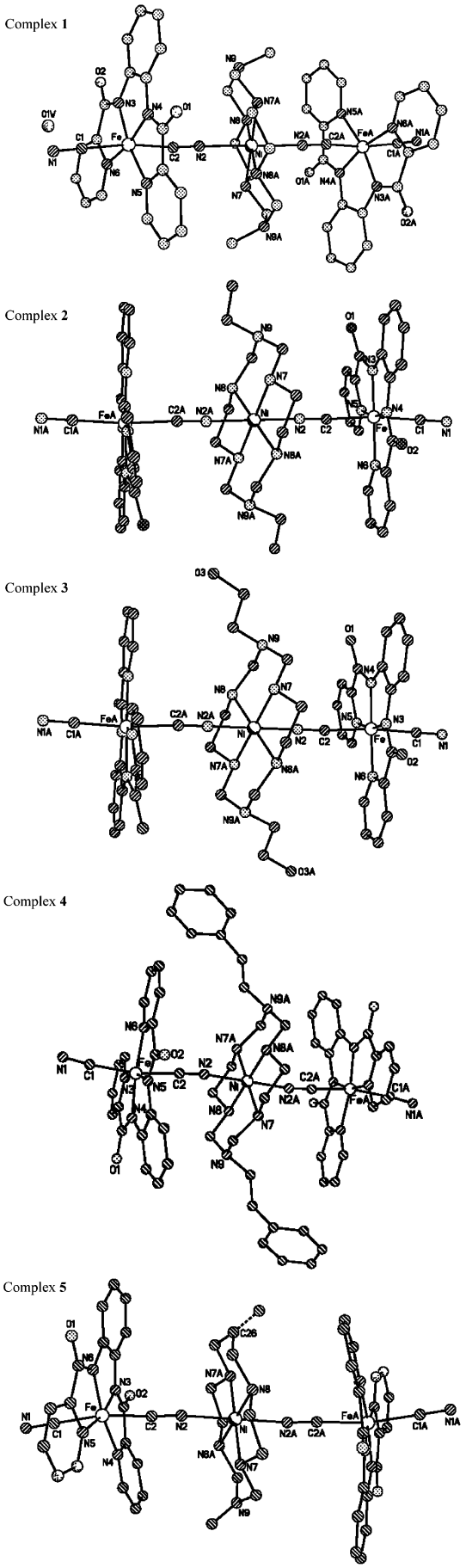

Figure 1. Crystal structures of trimeric $NiFe_2$ complexes **1**−**5**.

Table 3. Selected Bond Distances (Å) and Angles (deg) for Complexes **6**−**8**[a]

6		**7**		**8**	
Ni−N(1)#1	2.166(2)	Ni(1)−N(1)	2.133(7)	Ni(1)−N(1)	2.122(4)
Ni−N(7)	2.091(3)	Ni(1)−N(7)	2.076(8)	Ni(1)−N(7)	2.074(5)
Ni−N(8)	2.091(3)	Ni(1)−N(8)	2.059(7)	Ni(1)−N(8)	2.064(4)
Ni−N(2)	2.075(2)	Ni(2)−N(2)	2.109(9)	Ni(2)−N(2)	2.109(4)
Ni−N(9)	2.066(3)	Ni(2)−N(10)	2.059(8)	Ni(2)−N(10)	2.066(5)
Ni−N(10)	2.081(2)	Ni(2)−N(11)	2.049(9)	Ni(2)−N(11)	2.074(5)
Fe−C(1)	1.981(3)	Fe(1)−C(1)	1.981(9)	Fe(1)−C(1)	1.961(5)
Fe−C(2)	1.959(3)	Fe(1)−C(2)	1.956(11)	Fe(1)−C(2)	1.953(5)
Fe−N(3)	2.011(2)	Fe(1)−N(3)	2.005(9)	Fe(1)−N(3)	1.999(4)
Fe−N(4)	1.891(2)	Fe(1)−N(4)	1.898(9)	Fe(1)−N(4)	1.877(4)
Fe−N(5)	1.885(2)	Fe(1)−N(5)	1.884(9)	Fe(1)−N(5)	1.897(4)
Fe−N(6)	2.003(2)	Fe(1)−N(6)	2.015(9)	Fe(1)−N(6)	2.001(4)
Fe···Ni	5.048	Fe(1)···Ni(1)	5.088	Fe(1)···Ni(1)	5.184
Fe···Ni#1	5.144	Fe(1)···Ni(2)	5.197	Fe(1)···Ni(2)	5.193
N(1)−C(1)−Fe	170.6(2)	N(1)−C(1)−Fe(1)	169.3(8)	N(1)−C(1)−Fe(1)	174.5(4)
N(2)−C(2)−Fe	176.4(3)	N(2)−C(2)−Fe(1)	177.2(11)	N(2)−C(2)−Fe(1)	174.3(5)
C(1)−Fe−C(2)	175.16(12)	C(1)−Fe(1)−C(2)	174.9(4)	C(1)−Fe(1)−C(2)	166.4(2)
C(2)−N(2)−Ni	168.8(2)	C(2)−N(2)−Ni(2)	173.9(10)	C(2)−N(2)−Ni(2)	172.7(4)
C(1)−N(1)−Ni#2	150.1(2)	C(1)−N(1)−Ni(1)	156.3(7)	C(1)−N(1)−Ni(1)	166.7(4)
N(2)−Ni−N(1)#1	175.19(9)				

[a] Symmetry operations: #1, $-x, y + {}^1/_2, -z + {}^1/_2$; #2, $-x, y - {}^1/_2, -z + {}^1/_2$.

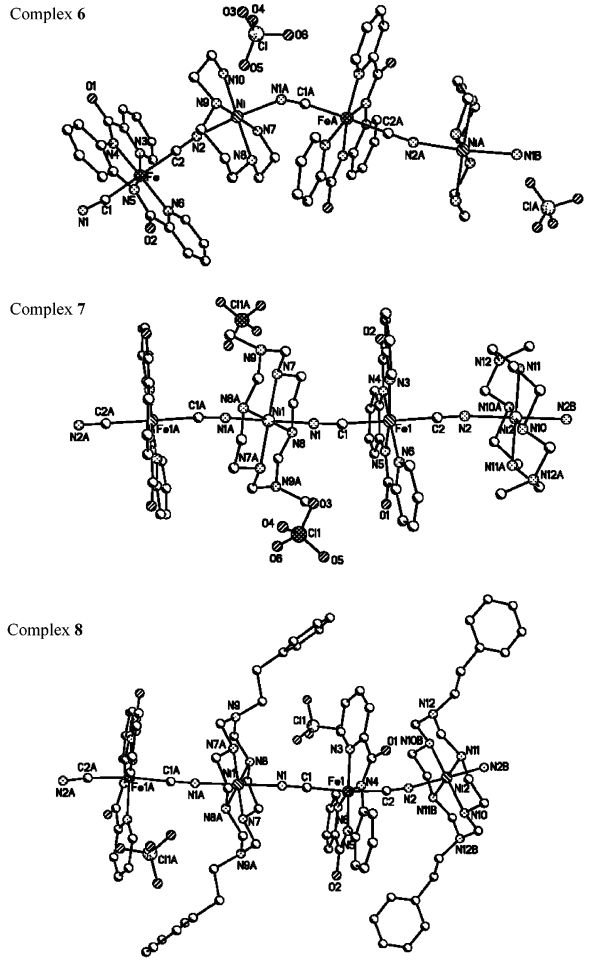

Figure 2. Crystal structures of 1D chainlike complexes **6**−**8**.

Ni−N≡C bond angles, the shorter the Ni−N_{cyano} bond distances and the longer the intramolecular Fe- - -Ni separations.

Crystal Structures of 1D Complexes 6, 7, and 8. X-ray crystallography of complexes **6**−**8** reveals that the structure consists of a one-dimensional cationic polymer $\{[NiL][Fe(bpb)(CN)_2]\}_n^{n+}$ (L = L^1, L^4, and L^6), with free ClO_4^- as counteranion (Figure 2). The wavelike chain is comprised of cyano-bridged alternating $[Fe(bpb)(CN)_2]^-$ and $[NiL]^{2+}$ fragments. In the chain, $[Fe(bpb)(CN)_2]^-$ uses two trans CN^- groups to connect with two $[NiL]^{2+}$ groups, whereas each $[NiL]^{2+}$ group is linked to two $[Fe(bpb)(CN)_2]^-$ ions in trans positions. Two nitrogen atoms of the bridging C≡N groups coordinate to the Ni(II) ions with the Ni−N contacts in the range 2.075(2)−2.166(2) Å and with Ni−N≡C bond angles ranging from 150.1(2)° for C(2)−N(2)−Ni(2) in complex **6** to 174.4(10)° for C(2)−N(2)−Ni(2) in complex **7**. The Fe−C distances in the three complexes range from 1.953(5) to 1.981(3) Å. The intramolecular Fe- - -Ni separations through bridging cyanides are 5.048, 5.097, and 5.184 Å for complexes **6**, **7**, and **8**, respectively. The shortest interchain metal−metal distances are 8.151, 8.781, and 7.577 Å in complexes **6**, **7**, and **8**, respectively.

The cell packing diagram (Figure 3) of complex **6** shows the H-bonding interaction between the two O atoms of one ClO_4^- ion between two chains and the two N atoms in L^6 from two adjacent chains, as well as that between the O atom located on bpb^{2-} and the N on L^6 from another adjacent chain. Thus, the H-bonded chains form a 3D network. In addition, there exists a hydrogen bond between O_{amide} in bpb^{2-} and the free methanol molecules.

Magnetic Properties of Trimeric Complexes 1, 3, 4, and 5. The temperature dependences of magnetic susceptibilities for the four complexes measured in the range 2−300 K under the external magnetic field of 1000 Oe are illustrated in Figure 4. The room-temperature values of $\chi_m T$ for the four complexes are in the range 1.94−2.01 emu K mol^{-1} and, due to spin−orbit coupling effects of low-spin Fe^{III}, are higher than the spin-only value of 1.75 emu K mol^{-1} expected for a magnetically dilute spin system (S_{Fe}, S_{Ni}, S_{Fe} = ${}^1/_2$, 1, ${}^1/_2$) with g = 2.00. The $\chi_m T$ values of the four complexes remain nearly constant until ∼200 K and then increase smoothly and attain a maximum value of 2.80 emu K mol^{-1} at 7.0 K for **1**, 3.07 emu K mol^{-1} at 6.0 K for **3**, 3.09 emu K mol^{-1} at 7.0 K for **4**, and 2.56 emu K mol^{-1} at

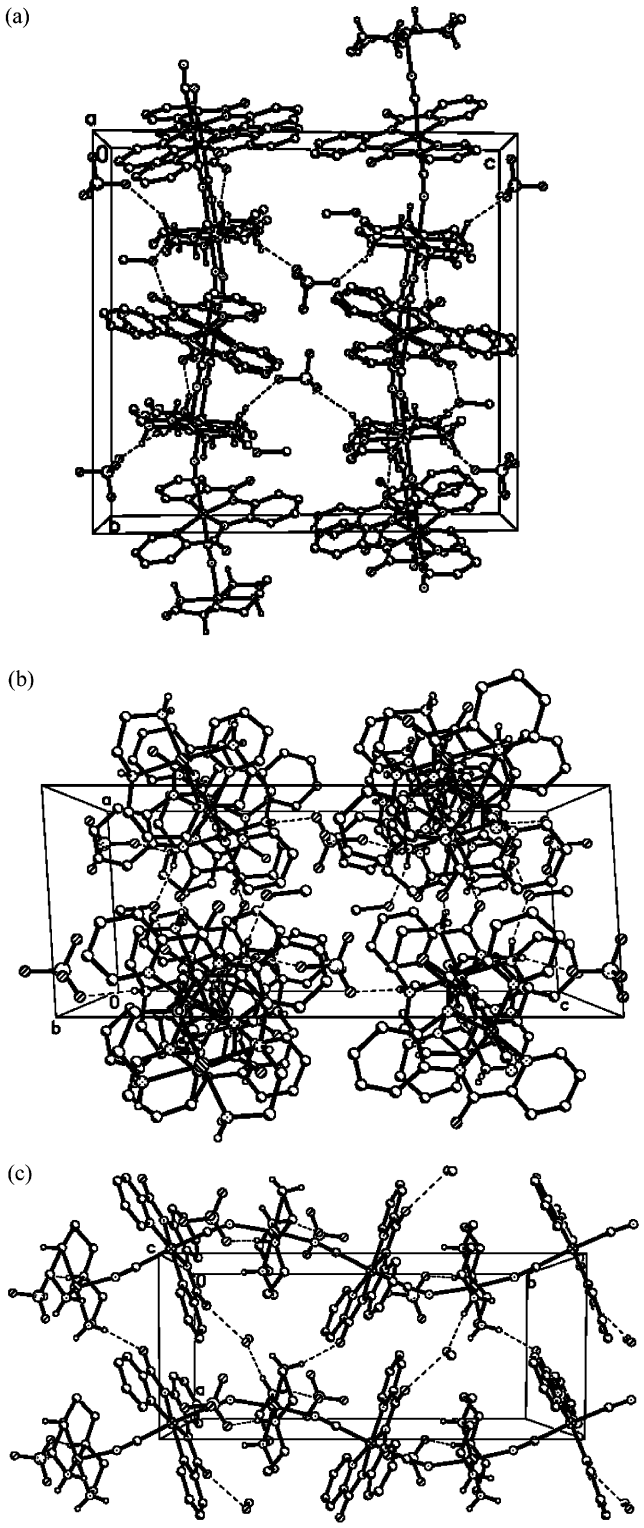

Figure 3. Interchain interactions in **6** (only the hydrogen atoms attached to the nitrogen atoms have been shown): (a) along the *a* axis, (b) along the *b* axis, (c) along the *c* axis.

9.0 K for **5**, which are close to the expected saturated value of 3.0 emu K mol^{-1} with the $S = 2$ ground state based on $g = 2.00$. The $\chi_m T$ values decrease rapidly and reach a value of 2.29, 2.96, 2.81, and 1.87 emu K mol^{-1} at 2.0 K for **1**, **3**, **4**, and **5**, respectively, which is probably due to the integrated operation of the saturation effect, the intermolecular antiferromagnetic interaction, and/or the zero-field-splitting (ZFS) effect of the Ni(II) ions. The magnetic susceptibilities obey Curie−Weiss law (inset of Figure 4) with a positive Weiss constant $\theta = +4.28$ K and Curie constant $C = 1.93$ emu K mol^{-1} for **1**, $\theta = +5.09$ K and $C = 1.97$ emu K mol^{-1} for **3**, $\theta = +5.62$ K and $C = 1.94$ emu K mol^{-1} for **4**, and $\theta = +3.26$ K and $C = 1.94$ emu K mol^{-1} for **5**; these values confirm the presence of overall ferromagnetic interactions in these complexes. These magnetic behaviors are consistent with an intramolecular Fe(III)−Ni(II) ferromagnetic interaction, which can be rationalized in terms of the strict orthogonality of the magnetic orbitals of the low-spin Fe(III) [d^5, t_{2g}^5] and Ni(II) [d^8, $t_{2g}^6 e_g^2$] centers, an arrangement which normally gives rise to ferromagnetic coupling. On the basis of the trimeric model, the magnetic susceptibilities can be fitted accordingly by the following expression derived from the exchange spin Hamiltonian $H = -2JS_{Ni}(S_{Fe(1)} + S_{Fe(2)})$:

$$\chi_m = \frac{2N\beta^2 g^2}{k(T-\Theta)} \frac{1 + 5\exp(4J/kT) + \exp(2J/kT)}{3 + 5\exp(4J/kT) + \exp(-2J/kT) + 3\exp(2J/kT)}$$

The best-fit parameters obtained are $J = +6.40(5)$ cm^{-1}, $g = 2.06(1)$, $\Theta = -0.77(1)$ K, and $R = \sum(\chi_{obsd}T - \chi_{cald}T)^2/\sum(\chi_{obsd}T)^2 = 1.23 \times 10^{-5}$ for **1**; $J = +7.8(1)$ cm^{-1}, $g = 2.06(1)$, $\Theta = -0.19(1)$ K, and $R = 2.44 \times 10^{-5}$ for complex **3**; $J = +8.9(2)$ cm^{-1}, $g = 2.05(1)$, $\Theta = -0.19(1)$ K, and $R = 7.51 \times 10^{-5}$ for complex **4**; and $J = +6.03(4)$ cm^{-1}, $g = 2.05(1)$, $\Theta = -1.43(1)$ K, and $R = 2.04 \times 10^{-5}$ for complex **5**, where Θ accounts for the contributions except intramolecular magnetic coupling.

Apparently, complexes **1**, **3**, **4**, and **5** exhibit similar magnetic properties. Comparison of the magnetic exchange parameters J with the Ni−N≡C bond angles for the four complexes is shown in Figure 5. The J values are approximately correlated to the Ni−N≡C bond angles: the larger the Ni−N≡C angle, the stronger the Ni- - -Fe magnetic interaction in this system. Therefore, it can be concluded that the *linear* bridging bond angle is a key factor in the *strong* intermetallic magnetic coupling. This is understandable, considering that linear bridging linkage results in better orbital overlap between the cyano nitrogen lone electron pair and the magnetic orbitals ($d_{x^2-y^2}$ and d_{z^2}) of Ni(II). A nearly linear best fit gives the correlation of $J_{NiFe} = 0.181\theta - 22.281$ cm^{-1}, where θ is the Ni−N≡C bond angle (deg). It should be pointed out that this correlation is rough and should be treated carefully because it does not include the effect of the Ni−N_{cyano} bond distances. Nevertheless, the variation trend of J_{NiFe} can be clearly seen, and the qualitative conclusion can be undoubtedly drawn.

Magnetic Properties of 1D Complexes 6−8. The magnetic susceptibilities of complexes **6**−**8** have been measured in the temperature range of 2−300 K for **6** and **8** and 5−300 K for **7** with a SQUID magnetometer. The $\chi_m T$ versus T plots of **6**−**8** are shown in Figures 6 and 10, where χ_m is the magnetic susceptibility/NiFe unit. On lowering the temperature, $\chi_m T$ increases smoothly, reaching a maximum value of 2.54 emu K mol^{-1} at 6.0 K for **6**, 2.45 emu K mol^{-1} at

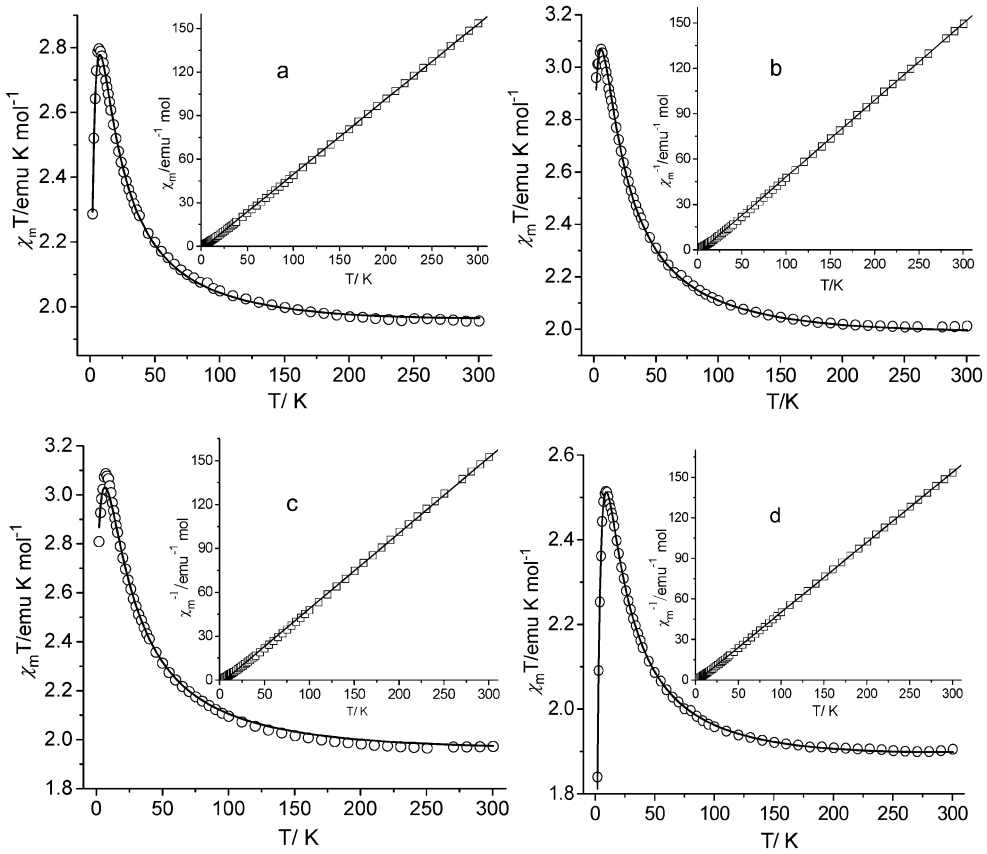

Figure 4. Temperature dependences of $\chi_m T$ and χ_m^{-1} (inset: the solid line was calculated from the Curie−Weiss law) for (a) **1**, (b) **3**, (c) **4**, and (d) **5**. The solid line represents the best fit based on the parameters discussed in the text.

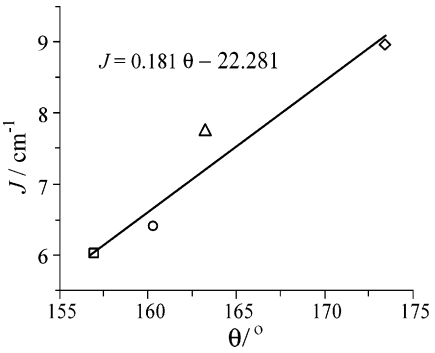

Figure 5. J_{NiFe} vs Ni−N≡C bond angle (θ) for **1** (○), **3** (△), **4** (◇), and **5** (□). The straight line is the best fit by using the equation shown in the plot.

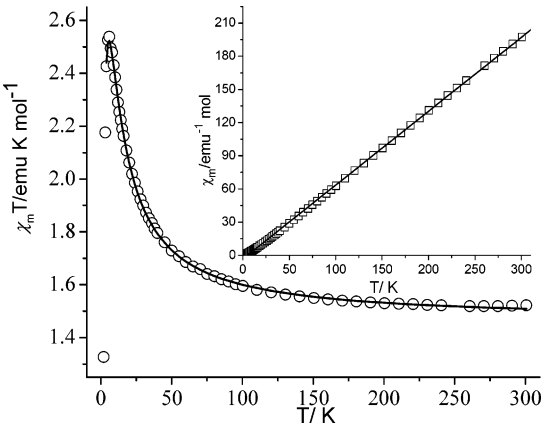

Figure 6. Temperature dependence of $\chi_m T$ and χ_m^{-1} (inset: the solid line was calculated from the Curie−Weiss law) for **6**. The solid line represents the best fit based on the parameters discussed in the text.

7.1 K for **7**, and 1.93 emu K mol^{-1} at 7.5 K for **8**, and then sharply decreases to 1.38 emu K mol^{-1} for **6** and 1.466 emu K mol^{-1} for **8** at 2 K. The magnetic susceptibilities of complexes **6**−**8** obey the Curie−Weiss law with positive Weiss constant $\theta = +4.97(1)$ K and Curie constant $C =$ 1.50(3) emu K mol^{-1} for **6**, $\theta = +5.92(1)$ K and $C = 1.50$-(1) emu K mol^{-1} for **7**, and $\theta = +3.27(1)$ K and $C = 1.47$-(1) emu K mol^{-1} for **8**. The positive Weiss constants and the increasing tendency of $\chi_m T$ above 7.5 K for the three complexes are typical of ferromagnetic coupling between adjacent Fe(III)−Ni(II) ions. The abrupt decrease at low temperature may be due to the operation of the magnetic saturation effect, weak interchain antiferromagnetic interactions, and the zero-field-splitting effect of the Ni(II) ions.

To analyze the magnetic data of **6**−**8**, we tried to use an approximate approach similar to that previously used for 1D complexes.[43] On the basis of the crystal data, the Fe(III)−CN−Ni(II) linkages are unequal. Therefore, the 1D chain can be treated as alternating uniform FeNi dimers with different intradimeric and intrachain (also interdimer) exchange constants (J_d vs J_c). A molecular field approximation was also included.

$$\chi_d = \frac{Ng^2\beta^2}{4kT}\frac{10 + \exp(-3J_d/kT)}{3 + \exp(5J_d/kT)} \qquad (1)$$

$$\chi_d = \frac{Ng^2\beta^2}{3kT} S_d(S_d + 1) \quad (2)$$

$$\chi_{chain} = \frac{Ng^2\beta^2}{3kT} \frac{1+u}{1-u} S_d(S_d + 1) \quad (3)$$

where $u = \text{cth}[J_c S_d(S_d + 1)/kT] - kT/(J_c S_d(S_d + 1))$

$$\chi_{chain} = \frac{\chi_m}{1 - \chi_m(2zJ'/Ng^2\beta^2)} \quad (4)$$

Using this model, the susceptibilities over the temperature range 4−300 K for **6**, 5−300 K for **7**, and 2−300 K for **8** were simulated, giving the best fits with parameters $J_c = +1.31(1)$ cm^{-1}, $J_d = +7.1(1)$ cm^{-1}, $zJ' = -1.21(1)$ cm^{-1}, $g = 2.06(1)$, and $R = 1.43 \times 10^{-5}$ for **6**; $J_c = +1.34(3)$ cm^{-1}, $J_d = +6.1(1)$ cm^{-1}, $zJ' = -1.02(3)$ cm^{-1}, $g = 2.08(1)$, and $R = 2.31 \times 10^{-5}$ for **7**; and $J_c = +0.591(7)$ cm^{-1}, $J_d = +7.49(9)$ cm^{-1}, $zJ' = -1.02(1)$ cm^{-1}, $g = 2.05(1)$, and $R = 9.92 \times 10^{-6}$ for **8**. The Ni(II)−Fe(III) exchange coupling parameters of these complexes are comparable to that of the cyano-bridged 1D Ni(II)−Cr(I) complex ($J_c = +0.23$, $J_d = +8.4$) as the result of similar C≡N−Ni linkages.[43]

Interestingly, magnetic susceptibility measurements of zero-static field ac magnetic susceptibilities for complex **6** at different frequencies confirm the long-range antiferromagnetic ordering below 3.5 K (Figure 7). The field-dependent magnetization was measured up to 50 kOe at 1.83 K (Figure 8). The curve has a sigmoid shape typical of metamagnetic behavior: the magnetization first increases slowly with increasing H until 6 kOe due to antiferromagnetic interchain interactions, then increases abruptly for a phase transition to a ferromagnetic state at about 10 kOe, and finally attains a saturation magnetization of 2.9 $N\beta$ (expected value: 3 $N\beta$ for $S_T = {}^3/_2$) at 50 kOe. The field-cooled magnetization (FCM) measurements (Figure 9) with the applied fields of 200 and 5000 Oe show a break at ∼3 K, which further demonstrates that there exists an antiferromagnetic phase transition at ∼3 K. The absence of a peak for the 10 kOe curve shows the metamagnetic behavior of the complex, and the critical field (H_c) to overcome the interchain antiferromagnetic interaction is less than 10 kOe.

Unlike the case for **6**, the field-cooled magnetization measurements for complexes **7** and **8** show the absence of magnetic ordering down to 2 K. The field dependence of magnetization (inset of Figure 10) for **7** and **8** shows no abnormity, indicative of the paramagnetic properties of the two complexes. The experimental data for **7** are consistent with the calculated Brillouin function that corresponds to $S_T = S_{Fe} + S_{Ni} = 1.5$ and are above that for the uncoupled $S_{Fe} = {}^1/_2$ and $S_{Ni} = 1$ state with $g = 2.11$, as shown in the inset of Figure 10. This clearly shows the ferromagnetic coupling between the adjacent Fe(III) and Ni(II) ions via the cyano bridges. However, the very low magnetization value (∼1.5 $N\beta$) at 50 kOe for compound **8** is far from saturation (3 $N\beta$ with $g = 2.0$) and is even lower than that for the uncoupled $S_{Fe} = {}^1/_2$ and $S_{Ni} = 1$ state, probably due to the presence of noticeable interchain antiferromagnetic interaction. Single-crystal X-ray diffraction analysis shows

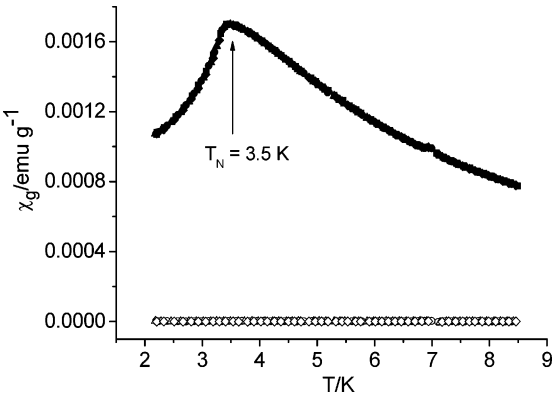

Figure 7. Temperature dependence of ac magnetization of **6** in a zero-static field and an ac field of 2 Oe at frequencies of 277, 666, 1633, and 4111 Hz.

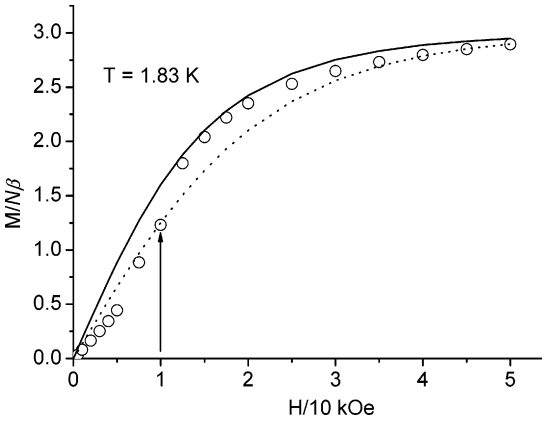

Figure 8. Field dependence of magnetization at 1.83 K for **6**. The solid or dotted line is the Brillouin curve for $S = {}^3/_2$ or for uncoupled $S_{Fe} = {}^1/_2$ and $S_{Ni} = 1$ with $g = 2.0$.

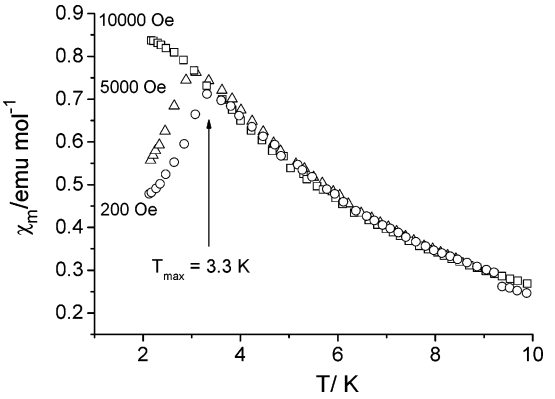

Figure 9. Field-cooled-magnetization of **6** in applied fields of 200 Oe, 5000 Oe, and 10 kOe.

that compound **8** has chains connected by ClO_4^- through H-bonding, giving rise to a layered structure (see Supporting Information). The layers are isolated from each other, however, by the bulky pendent benzene groups of the macrocyclic ligands. Hence, the low magnetization value of the compound at low temperatures is tentatively attributed to the probably strong intralayer antiferromagnetic magnetic interaction. The *isolated* layers are far apart, and the dipolar interaction is negligible, which precludes the occurrence of a 3D order.

The interchain antiferromagnetic interactions in the three 1D chainlike complexes are present, albeit weak, which

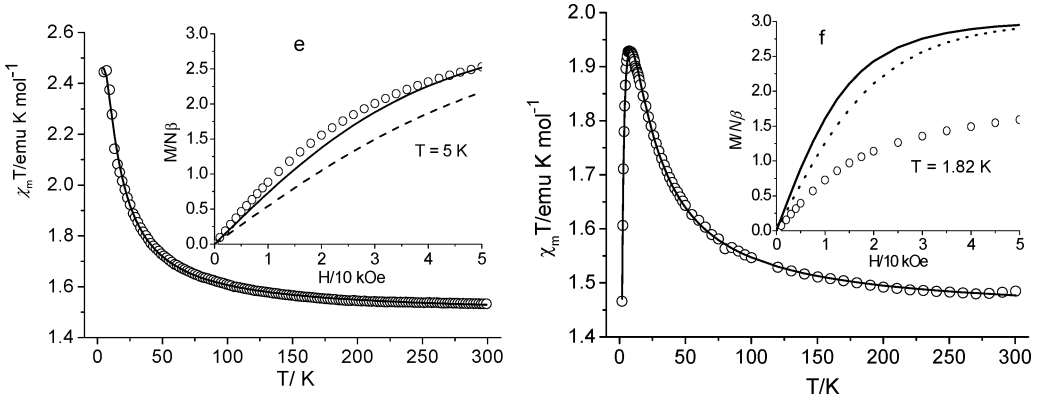

Figure 10. Temperature dependence of $\chi_m T$ with the fitting results for (e) **7** and (f) **8**. Inset: Field dependence of magnetization. The lines represent the Brillouin functions that corresponds to the uncoupled $S_{Fe} = {}^1/_2$ and $S_{Ni} = 1$ states (dotted lines) and $S_T = S_{Fe} + S_{Ni} = 1.5$ (solid lines) with $g = 2.11$ for **7** and $g = 2.0$ for **8**.

originates from the dipolar interaction and the hydrogen bonds as mentioned above for **6**. The interchain antiferromagnetic interactions may hinder the formation of SCMs, which require that the interchain antiferromagnetic interaction be negligibly weak. Similarly, the occurrence of 3D ordering in **6** requires comparatively strong interchain antiferromagnetic interactions. Therefore, the absence of a magnetic phase transition for **7** and **8** down to 2 K shows that the interchain antiferromagnetic interactions are not strong enough for 3D magnetic ordering.

Conclusions

The dicyano-containing $[Fe(bpb)(CN)_2]^-$ building block can react with the four-coordinate Ni(II) precursors to produce zero- or one-dimensional bimetallic complexes. Interestingly, the products strongly depend on the preparation methods. Magnetic investigation reveals that the magnitude of the Ni(II)—Fe(III) magnetic coupling is related to the bridging Ni—N≡C bond angles. It is anticipated that the formation of cyano-bridged 2D or 3D complexes is not likely because of the space hindrance of the bpb^{2-} ligand. Future work will involve the preparation of low-dimensional Mn(III)—Fe(III) complexes that may exhibit SCM or SMM behavior. Additionally, the employment of the analogous building block $[Cr(bpb)(CN)_2]^-$ will be studied. Results will be presented later.

Acknowledgment. This work was supported by the National Natural Science Foundation of China (Project Nos.: 20201008 and 50272034) and Fok Ying Tong Education Foundation.

Supporting Information Available: Cell packing diagrams for **8**. An X-ray crystallographic file (CIF). This material is available free of charge via the Internet at http://pubs.acs.org.

IC0489903